Ultrasonics 95 (2019) 32–36

Contents lists available at ScienceDirect

Ultrasonics

journal homepage: www.elsevier.com/locate/ultras

Long-distance shift of ultrasonic beam using a thin plate with periodic gratings

Dan Li[a,1], Xu Yan[b,1], Zheng Xu[b], Dean Ta[a]

[a] Department of Electronic Engineering, Fudan University, Shanghai 200433, China
[b] Institute of Acoustics, Tongji University, Shanghai 200092, China

ARTICLE INFO

Keywords:
Ultrasonic beam shift
Schlieren imaging
Guided waves
Finite-element method

ABSTRACT

We achieved the shift of ultrasonic beam over a long distance by guided waves through a brass plate with two groups of periodical gratings on the surface. Using Schlieren imaging, we experimentally observed the propagation of ultrasonic waves through this structure. In addition, simulations were performed using the finite-element method. Both the experimental and simulation results revealed that the shift of ultrasonic beam can be realized in this structure. We further investigated the effect of the shift distance and the size of the gratings on the shift efficiency, and discussed the mechanism. The proposed structure has potential applications in non-destructive evaluation.

1. Introduction

Ultrasound has been widely used in various scientific fields due to its high directivity, high sensitivity, ease of operation and its ability to propagate in a solid. Nowadays, it has been used in chemistry [1–3] and biology [4–6], as well as in medicine and numerous industries [7,8]. To broaden the application of ultrasound, varied strategies have been applied to manipulate ultrasonic beams. For example, phononic crystals have been used to realize ultrasound negative refraction [9], focusing [9,10], tunneling [11], and, more recently, transportation of acoustic energy by using the acoustic valley Hall phase [12]. However, phononic crystals are based on scattering or local resonance, and thus require a certain thickness to operate efficiency, which limits their practical application. In the audible sound range, metasurfaces have been proposed to decrease the thickness of the structure for manipulating sound waves [13–15]. However, it is difficult to extend this theory to the ultrasonic range, because the metasurface structure should generally be far smaller than the wavelength of the sound, which represents a significant fabrication challenge.

Ultrasound beam shift is attracting growing attention. Breazeale et al. realized ultrasound beam shift by incidence of ultrasonic waves at the Rayleigh angle onto a liquid solid interface [16]. Zeng et al. theoretically calculated the shift of acoustic wave at interface between double-positive and double-negative media [17]. Shift of ultrasound beam by use of plate has been also investigated by Xu et al. However, the space-shift of the leaky wave is very limited, and is generally frequency-dispersed, which prevents the energy from being concentrated [18].

In recent years, ultrasound propagation through periodic structures on plates has been widely investigated. For example, enhancement of ultrasound transmission was achieved using periodic gratings on plates [19,20]. In addition, ultrasound waveguiding and frequency selection of Lamb waves was achieved using a grating plate [21]. Chen et al. report the concept of a gradient piezoelectric self-sensing system by integrating shunting circuitry into conventional sensors [22]. Zhu et al. proposed a design based on kirigami to control subwavelength flexural waves propagating in a thin substrate structure [23]. Zhu and his co-worker further reviewed the plate-type elastic metamaterial and their potential applications [24]. Gratings on a plate have also been used to realize one-way transmission of ultrasound waves [25,26]. Moreover, the radiation force generated by ultrasound on a grating plate can be used to trap particles [27–29].

Despite the various studies using plate gratings, realization of ultrasonic beam shift through such structures has never been investigated. Ultrasound can propagate along a plate in the form of Lamb waves, the mode of the Lamb waves is widely used in non-destructive testing in industry. To excite the Lamb wave mode, the transmitter has to adjust to a precise incident angle, and the excited mode is commonly a combination of multiple modes. Furthermore, the receptor has to stick on the plate to examine the Lamb wave. By contrast, as we show in this article, by using a plate with periodic gratings, we are able to realize ultrasonic beam shift over a long distance. We performed Schlieren

E-mail addresses: gotoxvzheng@tongji.edu.cn (Z. Xu), tda@fudan.edu.cn (D. Ta).
[1] These authors contributed equally to this work.

https://doi.org/10.1016/j.ultras.2019.03.008
Received 22 September 2018; Received in revised form 6 March 2019; Accepted 6 March 2019
Available online 07 March 2019
0041-624X/

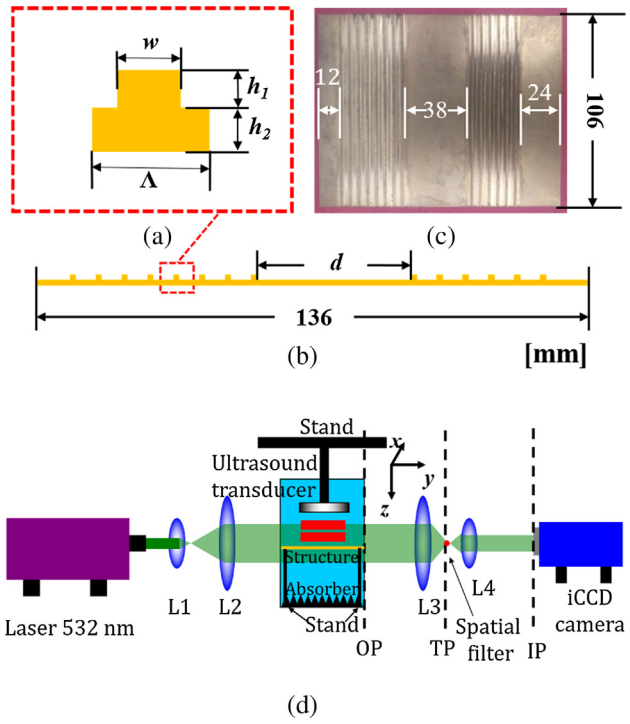

Fig. 1. (a) Side and (b) top view of the sample structure. (c) Photograph of the sample. (d) Schematic diagram of the Schlieren imaging system.

imaging of ultrasound propagation and discuss the mechanism of beam shift in this structure.

2. Methods

2.1. Periodic structure

The periodic structure used was a brass plate with intermittent periodic rectangles on one side. The dimensions of the structure are shown in a schematic diagram (Fig. 1(a) and (b)) and photograph (Fig. 1(c)). The width (w) and height (h_1) of the rectangle on the plate are 1 and 0.6 mm, respectively. The thickness (h_2) of the plate without the rectangle is 0.7 mm. The period (Λ) of the structure is 3.7 mm. There are two groups of rectangles on the plate. The distance (d) between two groups of rectangles is 38 mm. The Youngs' modulus, Poisson's ratio and density of the brass is 100 GPa, 0.34 and 8430 kg m^{-3}, respectively. The structure is immersed in water. The sound speed and the density of water were 1482 m s^{-1} and 998 kg m^{-3}, respectively.

2.2. Theoretical calculation

The propagation of elastic waves along a free, uniform plate of infinite length is described by the relation between the wave number (k_p) and the angular frequency (ω_p) through the Rayleigh–Lamb equation [30]:

$$\frac{\omega_p^4}{v_T^4} = 4k_p^2 q_2^2 \left(1 - \frac{q_1}{q_2}\frac{\tan(q_1 h_2/2)}{\tan(q_2 h_2/2)}\right), \text{ with } q_1^2 = \frac{\omega_p^2}{v_L^2} - k_p^2,\ q_2^2 = \frac{\omega_p^2}{v_T^2} - k_p^2 \quad (1)$$

The longitudinal and shear wave velocities are expressed as v_L and v_T, respectively.

2.3. Experimental

Visualization of the ultrasound field was conducted using the Schlieren method, which is based on the acousto-optic effect. A schematic diagram of the experimental setup is shown in Fig. 1(d). A laser beam (532 nm, DPGL-2150F, Photop, China) was expanded as a collimated light beam 75 mm in diameter using lenses L1 and L2, which were incident to the acoustic field. The acoustic field was generated in a transparent rectangular water tank made of quartz glass with dimensions of 120 × 120 × 200 mm^3 (width × length × height). To visualize the acoustic field, a circular plate, which blocked zero-order diffraction light, was placed on the transform plane. An intensified charge-coupled device (iCCD) camera (iStar DH734-18U-03, Andor, UK) was placed on the imaging plane to record the image, as illustrated in Fig. 1(d). The exposure time is fixed at 10 ns. Moreover, to ensure accuracy of the results, we used the average value of two measurements [31]. In this experiment, a commercial transducer (V301SU, Panametrics, Olympus) with a radius of 12.7 mm was used to generate a planar beam at a frequency of 271 kHz. The periodic structure was placed 40 mm below the transducer. It should be noted that the ultrasonic fields generated by the round ultrasound transducer is a circular planar wave field. However, the Lamb wave can be successfully excited since the diameter of the transducer covers about 8 period of the gratings.

Numerical simulations were conducted using the finite-element method (COMSOL Multiphysics, COMSOL AB, Stockholm, Sweden).

3. Results and discussion

Fig. 2(a) shows the phase velocities (v_p) of the Lamb modes in the plate obtained from the numerical results of Eq. (1). For the A_0 mode, the phase velocity of the Lamb wave is 1013 m/s at an ultrasound frequency being 271 kHz. Therefore, the wavelength is about 3.7 mm, which is the period of our structure. As shown in Fig. 2(a), a group of periodic rectangles is placed on the left side of the plate, and the

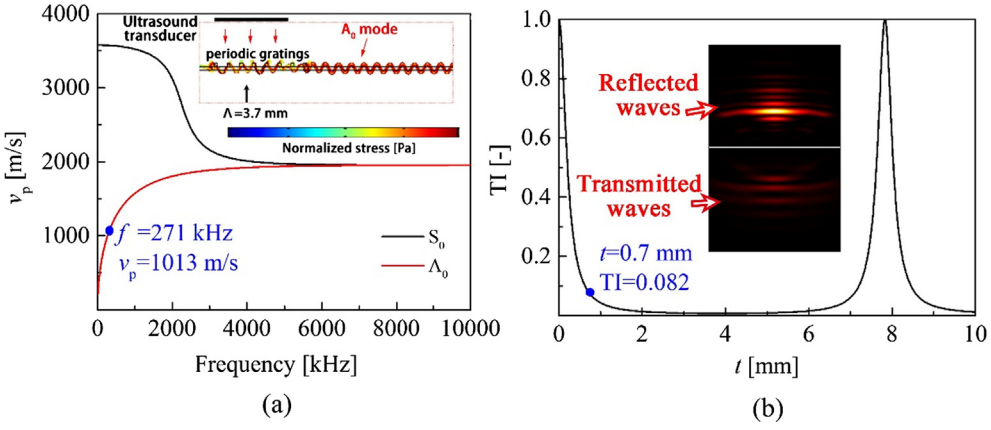

Fig. 2. (a) Dispersion curve and (b) transmittance of the plate.

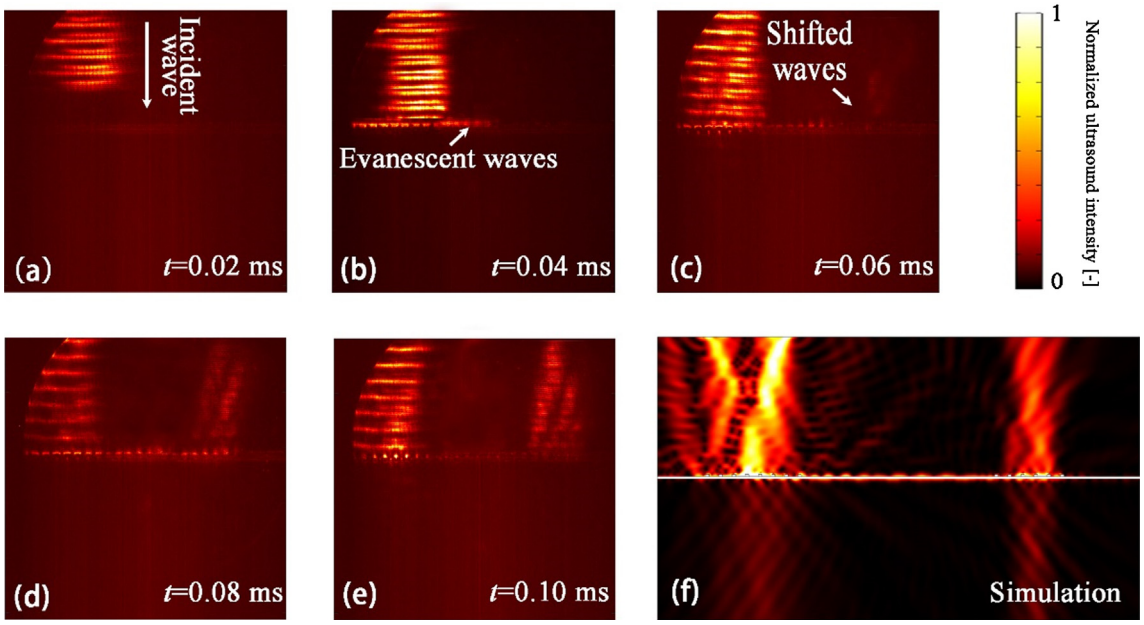

Fig. 3. (a–e) Experimental results and (f) simulation result for ultrasonic beam shift in our periodic structure.

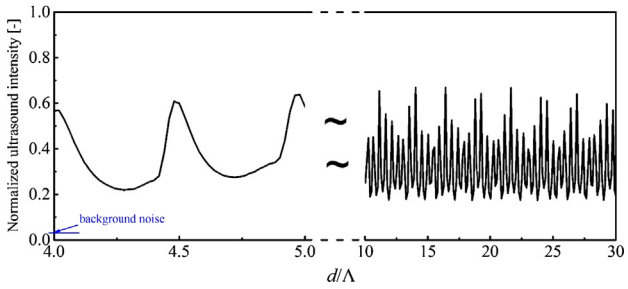

Fig. 4. Simulation results of the distance of the beam shift on the ultrasound intensity.

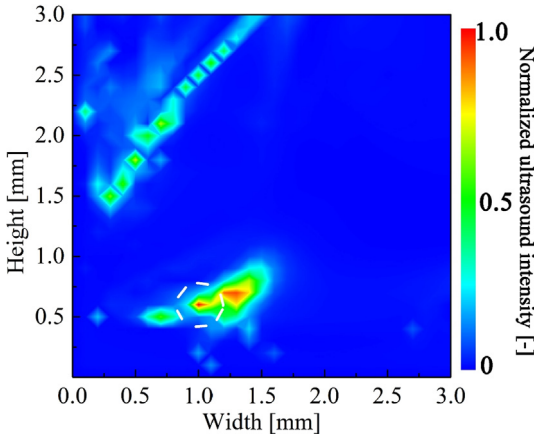

Fig. 5. Effect of the width and the height of the rectangles on the intensity of the beam shift.

ultrasound irradiates from its upper side. The A_0 mode vibration is excited in the plate, which can be observed from the scaled displacement of the plate. Then, we calculated the intensity transmission coefficient, which is defined as the ratio of the transmitted to the incident ultrasound intensity without gratings; the results are shown in Fig. 2(b). The results indicate that the intensity transmission coefficient is only 0.082 for $h_2 = 0.7$ mm. We further simulated a burst with 10 pulses of ultrasound propagation through the plate and the results are also shown in Fig. 2(b). It can be observed that the intensity of the transmitted waves is far lower than that of the reflected waves. By comparing Fig. 2(a) and (b), we deduced that by using periodic gratings, the ultrasound energy can be received by the plate and converted to Lamb waves owing to the A_0 resonance in the plate. This is because the waves arrived at surface of the rectangle and the plate is in the inverse phase. Furthermore, the period of the structure is the wavelength corresponding to the phase velocity. Therefore, the A_0 resonance can be easily excited.

Next, we experimentally investigated ultrasound propagation in this structure and the results are shown in Fig. 3. For comparison, the simulated ultrasound intensity distribution in the frequency domain is also given (Fig. 3(f)). It is observed that the ultrasound is incident on the plate from the left side (Fig. 3(a)) and propagates along the plate (Fig. 3(b)). At $t = 0.06$ ms, shifted waves are emitted from the right side of the plate (Fig. 3(c)), and the wave vector of the shifted waves is almost perpendicular to the plate (Fig. 3(d) and (e)). In contrast to the simulation results (Fig. 3(f)), in the experiment, we hardly observed the transmitted waves. This is possibly because the light intensity for the transmitted waves was below the detection threshold of the iCCD camera. We also note that waves propagate near the boundary of the plate and water. Because the Lamb wave is nonleaky in the plate according to the Snell's law:

$$\frac{\sin\theta_1}{c_{water}} = \frac{\sin\theta_2}{c_p} \tag{2}$$

and c_p (1013 m/s) is smaller than the c_{water} (1482 m/s). The wavenumber along the z axis can be calculated as

$$k_{1z}^2 = k_1^2 - k_{1x}^2 = k_1^2(1 - \sin^2\theta_1) \tag{3}$$

where k_1 is the wavenumber in water. The components of k_1 along the x and z axes are expressed as k_{1x} and k_{1z}. By substituting Eq. (2) into Eq. (3) and with θ_2 set to 90° because c_p propagates along the x axis, the calculated k_{1z} becomes an imaginary number. The ultrasound pressure (p) can be expressed as

$$p = p_a e^{i(k_{1x}x + k_{1z}z - \omega t)} \tag{4}$$

where p_a is the pressure amplitude. Thus, the attenuation coefficient (α) along the z axis becomes

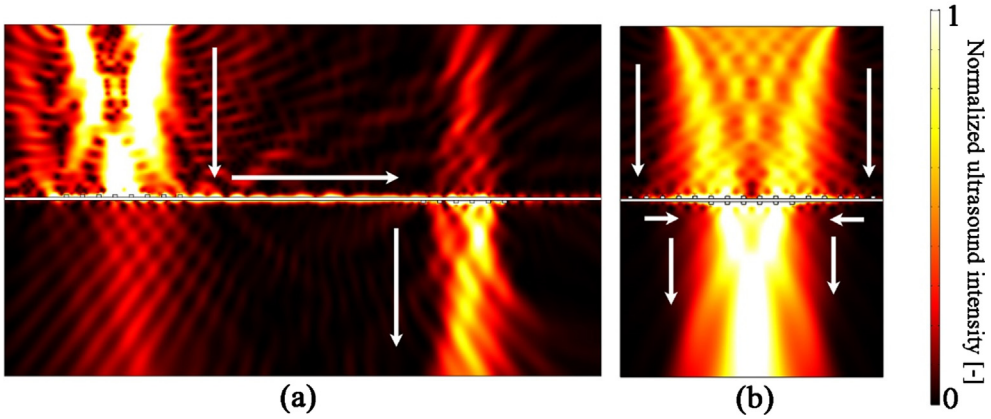

Fig. 6. (a) Ultrasonic beam shift on the reverse side. (b) Concentration of energy using a beam with broad beamwidth.

$$\alpha = k_1 \sqrt{\frac{c_{water}}{c_p} - 1} \tag{5}$$

Therefore, there are evanescent waves on the plate and the ultrasound pressure quickly attenuates along the z axis. It should also be noted that the incident and outgoing ultrasound waves both rely on the A_0 resonance with the periodic rectangles.

We numerically investigated the influence of distance between the two groups of rectangles on the ultrasound intensity and the results are shown in Fig. 4. When we varied the distance of the gratings, the emitted waves shifted accordingly. To avoid the sidelobe of the incident waves influencing the shifted waves, the start distance was set as $d/\Lambda = 4$. The shifted beam intensity was normalized with respect to the incident ultrasound intensity. The maximum shifted beam intensity was 0.6. Even the minimum intensity of 0.2 was much higher than the average ultrasound intensity in the background noise (0.02). The maximum shifted beam intensity occurred at the position d, which is an integer number of half the wavelength. In this situation, the plate between the two groups of rectangles becomes an acoustic resonator (*i.e.* the Fabry–Pérot condition [32]) and the shifted beam intensity reaches a maximum value. We note that the shifted beam intensity did not decrease even when d was 30 times the value of Λ, which further proves that Lamb waves are nonleaky in the plate in this structure and are able to shift ultrasonic beam over a long distance.

We investigated the effect of the width and the height of the rectangles on the intensity of the transmitted ultrasound and the results are shown in Fig. 5. In most cases, the energy of the shifted ultrasonic beam is nearly zero, which indicates that almost no energy can be transported in this structure. The maximum shifted beam occurred for a width and height of 1 and 0.6 mm, respectively. To excite the most-efficient A_0 mode in the plate, the height of the rectangle should be approximately equal to the thickness of the plate. In this situation, the waves reaching the surface of the rectangles and the plate are almost in the inverse phase, and the A_0 mode can be easily excited. Considering the waves propagating through the plate, the structure can be treated as a one-dimensional phononic-crystal passband when the width of the rectangle is 1 mm. Another relatively high-efficiency transport region, shown in the upper-left corner of Fig. 5, is also a passband for A_0 waves. However, the A_0 waves are not excited at high efficiency, thus reducing ultrasonic beam shift.

We also note that the structure can emit ultrasound waves from the reverse side of the plate if the periodic rectangles are placed on the reverse side. The simulation result is shown in Fig. 6(a). Another consideration is the enhancement of transmitted waves by the periodic rectangles. As shown in Fig. 6(b), we examined ultrasound irradiation from a beam with broad beamwidth from the upper side, with the periodic rectangles on the upper side of the plate covering the beamwidth. The number of periodic rectangles below the plate was lower than on the upper side. Thus, the ultrasound waves on both sides propagate to the center of the plate. As a result, the beamwidth decreases and the ultrasound intensity increases. In our future work, we will change the angle of the outgoing waves using periodic rectangles of different heights. We will also aim to further increase the intensity of the shifted beam.

4. Conclusion

In conclusion, we proposed a structure to achieve ultrasonic beam shift using periodic rectangles on a plate. We experimentally observed the ultrasonic waves propagating through the structure and discussed the mechanism. We discussed the effect of the distance between two groups of rectangles on ultrasound propagation. Moreover, we calculated the height and width of the rectangles needed to maximize the efficiency of energy transport. In contrast with other methods to manipulate the ultrasonic beam, our proposed structure has a negligible thickness. Because of its ease of fabrication, we believe that our structure has potential applications in non-destructive evaluation.

Acknowledgments

We thank Prof. Menglu Qian at Tongji University for helpful discussion on evanescent waves and Prof. Zhongqing Su at the Hong Kong Polytechnic University for helpful advice. This work was supported by the National Natural Science Foundation of China (Nos. 11774263, 11604055, 11674249 and 11525416), the National Key Research and Development Program of China (No. 2016YFA0100800), and the Fundamental Research Funds for the Central Universities. We thank Dr. Adam Brotchie from Edanz Group (www.edanzediting.com/ac) for editing a draft of this manuscript.

References

[1] S. Koda, T. Kimura, H. Mitome, Ultrason. Sonochem. 10 (3) (2003) 149–156.
[2] Z. Xu, K. Yasuda, X. Liu, Ultrason. Sonochem. 32 (2016) 241–246.
[3] Z. Xu, K. Yasuda, S. Koda, Ultrason. Sonochem. (2013) 452–459.
[4] D. Ta, W. Wang, Y. Wang, L. Le, Y. Zhou, Ultrasound Med. Biol. 35 (4) (2009) 641–652.
[5] G. Haar, D. Sinnett, I. Rivens, Phys. Med. Biol. 34 (10) (1989) 1743–1750.
[6] X. Song, D. Ta, W. Wang, Ultrasound Med. Biol. 37 (10) (2011) 1704–1713.
[7] J. Chen, Z. Su, L. Cheng, Smart Mater. Struct. 19 (2010) 015044-1–12.
[8] B. Drinkwater, P. Wilcox, NDT&E Int. 39 (2006) 525–541.
[9] A. Sukhovich, L. Jing, J. Page, Phys. Rev. B 77 (1) (2008) 014301-1-9.
[10] S. Yang, J. Page, Z. Liu, M. Cowan, C. Chan, P. Sheng, Phys. Rev. Lett. 93 (2) (2004) 024301-1-4.
[11] S. Yang, J. Page, Z. Liu, M. Cowan, C. Chan, P. Sheng, Phys. Rev. Lett. 88 (10) (2002) 104301-1-4.
[12] J. Lu, C. Qiu, L. Ye, X. Fan, M. Ke, F. Zhang, Z. Liu, Nat. Phys. 13 (2017) 369–374.
[13] G. Ma, M. Yang, S. Xiao, Z. Yang, P. Sheng, Nat. Mater. 13 (2014) 873–878.
[14] Y. Xie, W. Wang, H. Chen, A. Konneker, B. Popa, S. Cummer, Nat. Commun. 5 (2014) 5553-1-5.

[15] Y. Cheng, C. Zhou, B. Yuan, D. Wu, Q. Wei, X. Liu, Nat. Mater. 14 (2015) 1013–1019.
[16] M. Breazeale, L. Adler, G. Scott, J. Appl. Phys. 48 (1977) 530–537.
[17] L. Zeng, R. Song, Phys. Lett. A 358 (2006) 484–486.
[18] Z. Xu, M. Qian, Q. Cheng, X. Liu, Chin. Phys. Lett. 33 (11) (2016) 114302-1-4.
[19] Z. He, H. Jia, C. Qiu, S. Peng, X. Mei, F. Cai, P. Peng, M. Ke, Z. Liu, Phys. Rev. Lett. 105 (2010) 074301-1–4.
[20] Z. Hou, B. Assouar, J. Phys.: Appl. Phys. 41 (2008) 095103-1–7.
[21] T. Wu, T. Wu, J. Hsu, Phys. Rev. B 79 (2009) 104306-1–6.
[22] Y. Chen, R. Zhu, M. Barnhart, G. Huang, Sci. Rep. 6 (2016) 35048-1–11.
[23] R. Zhu, H. Yasuda, G. Huang, J. Yang, Sci. Rep. 8 (1) (2018) 483–493.
[24] R. Zhu, X. Liu, G. Hu, F. Yuan, G. Huang, Int. J. Smart Nano Mater. 6 (1) (2015) 14–40.
[25] J. Chen, X. Han, G. Li, J. Appl. Phys. 113 (2013) 184506-1–6.
[26] Z. Xu, W. Xu, X. Yan, M. Qian, Q. Cheng, Appl. Phys. Express 11 (2018) 027301-1 4.
[27] F. Li, F. Cai, Z. Liu, L. Meng, M. Qian, C. Wang, Q. Cheng, M. Qian, X. Liu, J. Wu, J. Li, H. Zheng, Phys. Rev. Appl. 1 (2014) 051001-1 5.
[28] T. Wang, M. Ke, S. Xu, J. Feng, C. Qiu, Z. Liu, Appl. Phys. Lett. 106 (2015) 163504.
[29] T. Wang, M. Ke, C. Qiu, Z. Liu, J. Appl. Phys. 119 (2016) 214502.
[30] Z. Xu, W. Xu, M. Qian, Q. Cheng, X. Liu, Ultrasonics 80 (2017) 66–71.
[31] Z. Xu, H. Chen, X. Yan, M. Qian, Q. Cheng, Opt. Express 25 (17) (2017) 20401–20409.
[32] Y. Takakura, Phys. Rev. Lett. 86 (2001) 5601.